

Polar distortions in hydrogen-bonded organic ferroelectricsAlessandro Stroppa,^{1,*} Domenico Di Sante,² Sachio Horiuchi,^{3,4} Yoshinori Tokura,^{5,6} David Vanderbilt,⁷ and Silvia Picozzi¹¹CNR-SPIN, L'Aquila, Italy²University of L'Aquila, Physics Department, Via Vetoio, L'Aquila, Italy³National Institute of Advanced Industrial Science and Technology (AIST) Tsukuba, Ibaraki 305-8562, Japan⁴CREST, JST, Tsukuba 305-8562, Japan⁵Department of Applied Physics, The University of Tokyo Hongo Bunkyo-ku, Tokyo 113-8656, Japan⁶Correlated Electron Research Group, RIKEN Advanced Science Institute, Wako 351-0198, Japan⁷Department of Physics and Astronomy, Rutgers University, 136 Frelinghuysen Road, Piscataway, New Jersey 08854-8019, USA

(Received 4 May 2011; published 15 July 2011)

Although ferroelectric compounds containing hydrogen bonds were among the first to be discovered, organic ferroelectrics are relatively rare. The discovery of high polarization at room temperature in croconic acid [Horiuchi *et al.*, *Nature (London)* **463**, 789 (2010)] has led to a renewed interest in organic ferroelectrics. We present an *ab initio* study of two ferroelectric organic molecular crystals, 1-cyclobutene-1,2-dicarboxylic acid (CBDC) and 2-phenylmalondialdehyde (PhMDA). By using a distortion-mode analysis we shed light on the microscopic mechanisms contributing to the polarization, which we find to be as large as 14.3 and 7.0 $\mu\text{C}/\text{cm}^2$ for CBDC and PhMDA, respectively. These results suggest that it may be fruitful to search among known but poorly characterized organic compounds for organic ferroelectrics with enhanced polar properties suitable for device applications.

DOI: 10.1103/PhysRevB.84.014101

PACS number(s): 77.84.Jd, 71.15.Mb, 33.15.Fm

The property of polarization switchable by an applied external electric field, i.e., ferroelectricity, is the basis of a wide range of device applications.¹ The first known ferroelectric material, discovered in 1920, was sodium potassium tartrate tetrahydrate ($\text{NaKC}_4\text{H}_4\text{O}_6 \cdot 4\text{H}_2\text{O}$), better known as Rochelle salt.² Unfortunately it is also one of the most complicated ferroelectrics known to date, and research in this field soon focused on simpler ferroelectrics, such as phosphates and arsenates, discovered later.^{3,4} A prototypical example is potassium dihydrogen phosphate, KH_2PO_4 , better known as KDP.⁵ The latter contains hydrogen bonds for which different possible arrangements of the hydrogens can result in different orientations of the dipolar units. After the discovery of ferroelectricity in BaTiO_3 , with polarizations as large as 27 $\mu\text{C}/\text{cm}^2$ in the tetragonal phase,⁶ attention switched to this new class of perovskite oxygen octahedral ferroelectrics made up from basic BO_6 building blocks, of which BaTiO_3 was the forerunner. These perovskite and related materials are by far the most investigated class of ferroelectrics, and the most important for current device applications. Nevertheless, substantial efforts are now being made in order to find ferroelectric materials that are potentially cheaper, more soluble, less toxic, lighter, or more flexible.^{7,8} Proton ordering in hydrogen-bonded systems has long been one of the central topics in condensed-matter physics.⁹ Very recently it was discovered that organic crystals of croconic acid, $\text{H}_2\text{C}_5\text{O}_5$, exhibit ferroelectricity with a large spontaneous polarization of 21 $\mu\text{C}/\text{cm}^2$.¹⁰ Croconic acid consists of polar stacks of sheets of hydrogen-bonded molecules.¹¹ Upon application of an electric field, protons associated with one molecule cooperatively shift to a hydrogen-bonded neighbor, switching the molecular dipole and giving rise to a large polarization.¹² It seems likely that this physical mechanism may also occur in many other organic materials whose ferroelectric properties have yet to be discovered and characterized. *Ab initio* calculations are a suitable tool in

this case, as they can not only identify materials with large polarization, but also shed light on the mechanisms behind the polarization itself. Organic materials show also promising routes for multiferroicity, i.e., a combination of ferroelectric and magnetic properties in the same compound and for magnetoelectricity, i.e., the intriguing possibility of controlling the ferroelectric polarization by an applied magnetic field, and vice versa, controlling the magnetization by applying an electric field.^{13–15}

In this paper, we focus on 1-cyclobutene-1,2-dicarboxylic acid (CBDC, $\text{C}_6\text{H}_6\text{O}_4$) (Ref. 16) and 2-phenylmalondialdehyde (PhMDA, $\text{C}_9\text{H}_8\text{O}_2$).¹⁷ Initial x-ray diffraction studies of CBDC (Ref. 16) and PhMDA (Ref. 17) were performed only at room temperature for CBDC and at $T = 111$ K for PhMDA. It was only recently that unique measurements were extended to low temperature for CBDC and to room temperature for PhMDA,¹⁸ showing that both compounds are *ferroelectric* with Curie temperatures above 400 and 363 K, respectively. The observed spontaneous polarization (P_x, P_y, P_z) is as large as (0.4, 0, 2.8) and (0, 0, 9) $\mu\text{C}/\text{cm}^2$ for CBDC and PhMDA, respectively.¹⁸ The main purpose of the present study is to describe the ferroelectricity in these compounds based on *ab initio* calculations. We have found that for both materials, the main contribution to the polarization is a collective proton transfer between molecular units, hereafter denoted as an “intermolecular” hydrogen shift. This is basically the same main mechanism found in croconic acid. However, importantly, we have also introduced a partial mode analysis of the contributions to the ferroelectricity, and found that correlated intramolecular distortions also contribute significantly to the polarization.

First-principles density-functional theory calculations were performed using the Vienna *ab initio* simulation package (VASP).^{19,20} The Kohn-Sham equations were solved using the projector augmented-wave pseudopotentials and the Perdew-Burke-Ernzerhof (PBE) generalized gradient density

approximation to the exchange-correlation potential.²¹ We used a plane-wave cutoff of 400 eV and k -point meshes of (6,2,4) and (4,2,6) for CBDC and PhMDA, respectively. The Berry-phase method was employed to evaluate the crystalline polarization.^{22,23} All atomic positions were optimized until the forces were below 0.01 eV/Å. Test calculations were performed to estimate effects beyond the local density approximation by using the Heyd-Scuseria-Ernzerhof hybrid functional, which has shown to improve the description of solid-state systems.^{24–35} We also checked the van der Waals corrections^{36,37} as proposed within a density-functional framework. In both cases the changes in the magnitude of polarization were found to be less than a few percent, confirming the basic physics explained in the present work. A more extended discussion about corrections beyond local and semilocal functionals will be presented in a forthcoming publication.³⁸

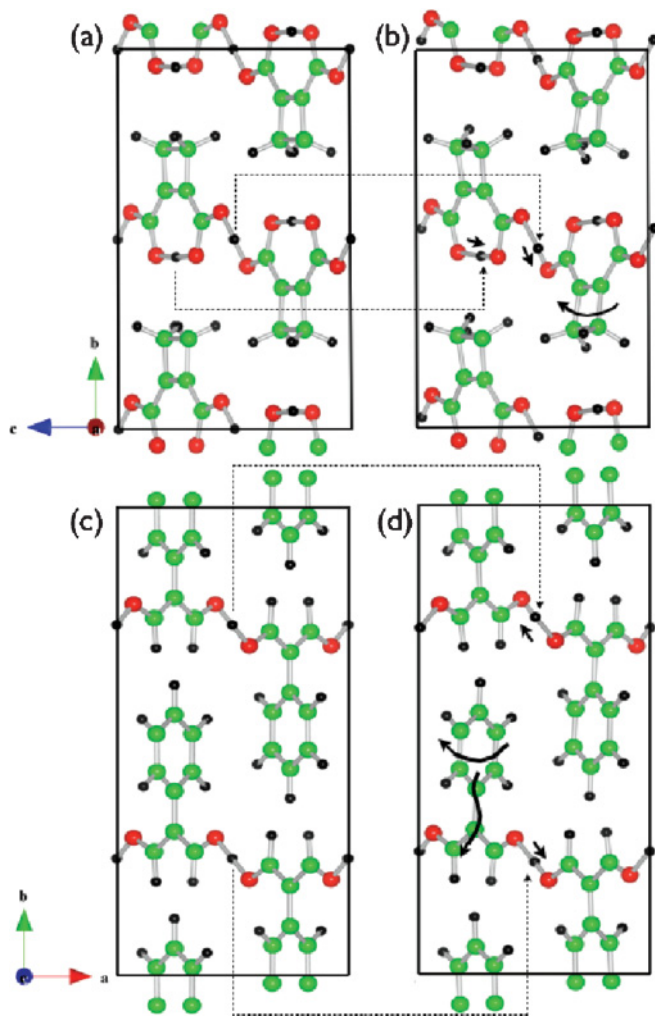


FIG. 1. (Color online) Ball-and-stick models of CBDC (top) and PhMDA (bottom). (a) and (c) refer to centric and (b) and (d) to polar structures. Dashed guiding-eye lines refer to the position of relevant hydrogens contributing to polarization; arrows in (b) and (d) indicate important polar distortions. Here and in Fig. 3, 4 green, red and black spheres are Carbon, Oxygen and Hydrogen atom.

In Fig. 1 we show a ball-and-stick model of CBDC (top) and PhMDA (bottom). In Figs. 1(a) and 1(c) we show the centric structures, and in Figs. 1(b) and 1(d) the polar ones. The CBDC molecular unit is formed by a main planar four-membered ring of carbon atoms similar to the planar cyclobutene molecule, and two carboxyl carbons, i.e., with formula $-\text{C}=\text{O}-\text{O}-\text{H}$, where “=” and “-” refer to double and single bonds. The molecular units shown in Fig. 1 are part of an infinite chain of molecules related by a glide plane and linked by intermolecular hydrogen bonds. The PhMDA molecular unit is formed by a planar phenyl group, i.e., six carbon atoms arranged in a planar ring, each of which is bonded to a H atom. The phenyl group is linked to a linear hydrogen-bonded chain of β -diketone enol moieties, i.e., $\text{O}(=\text{C})-\text{C}=\text{C}-\text{O}-\text{H}$. Hydrogen bonds link the molecules together along the $[102]$ and $[10\bar{2}]$ directions into infinite chains.

We found it useful here to introduce a pseudosymmetry analysis, in which a given low-symmetry (ferroelectric) structure is represented in terms of a symmetry-lowering Landau-type structural phase transition from a high-symmetry (paraelectric) parent structure, based on finding a supergroup of the given space group.^{39,40} CBDC crystallizes in the monoclinic space group Cc and its pseudosymmetric centric structure has space group symmetry $C2/c$; the two structures are related by a maximum atomic distortion of 0.43 Å. Analogously, PhMDA crystallizes in the $Pna2_1$ and its pseudosymmetric centric structure is $Pbcn$, with maximum atomic displacements of 0.25 Å. In order to gain insight into the ferroelectricity, we compare the relaxed centric and polar structures shown in Figs. 1(a) and 1(b) for CBDC and in Figs. 1(c) and 1(d) for PhMDA. For CBDC we have two types of hydrogen bonds (intramolecular and intermolecular) which, in the polar state, shift toward the molecular units on the right-hand side, as shown by the short arrows in Fig. 1(b). There is another cooperative atomic distortion, shown in Fig. 1(b) by the curved arrow, hereafter referred to as “molecular buckling.” For PhMDA, the hydrogen sitting between two molecular units in the polar structure shifts toward one of its neighboring units, as indicated by short arrows in Fig. 1(d). Two other relevant atomic distortions come into play, as shown by the curved arrows, both tending to deform the molecular units. One acts on the planar phenyl group, while the other distorts the β -diketone enol moieties. For both compounds, then, we find that three different types of distortion can contribute importantly to the ferroelectric polarization.

In Fig. 2 we show the variation of the total energy from the centric to the polar structure as a function of the amplitude of the polar mode. For both materials we find a bistable energy profile characteristic of a ferroelectric material with an energy barrier on the order of 0.3 eV/unit cell, suggesting that the polarization should be switchable upon application of an external electric field. For CBDC, the polarization is in the ac plane with a magnitude of $P = 14.3 \mu\text{C}/\text{cm}^2$, while for PhMDA it is along the c axis and equal to $7.0 \mu\text{C}/\text{cm}^2$. (Recall that the polarization of croconic acid is $21 \mu\text{C}/\text{cm}^2$.) The slight discrepancy with experimental values on CBDC might be due to insufficient optimization of high-quality crystallization.¹⁸ We next consider the relaxed structures of the high- and low-symmetry phases, analyzing the displacive-type transition between the two phases in terms of symmetry modes using

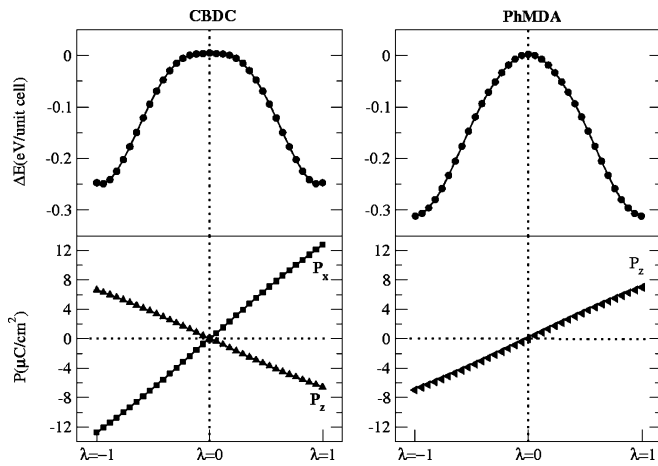


FIG. 2. Variation of total energy (top) and of polarization (bottom) as a function of the amplitude of the polar distortion between centric ($\lambda = 0$) and polar ($\lambda = \pm 1$) configurations.

the AMPLIMODES software package⁴¹ and ISODISTORT.⁴² The programs determine the global structural distortion that relates the two phases, enumerates the symmetry modes compatible with the symmetry breaking, and decomposes the total distortion into amplitudes of these orthonormal symmetry modes.

In Fig. 3 we show the centric structures for CBDC (left-hand side) and PhMDA (right-hand side), with the characteristic atomic displacements of the different polar distortion modes shown by arrows. As the polar mode acts separately on different Wyckoff positions (WPs) of the high-symmetry structure, it is meaningful to consider the action of the polar distortion on atoms belonging to different WPs separately. We denote these as $A(WP)$, and they are shown from top to bottom in Fig. 3. For CBDC, we have $A(4e)$ and $A(4b)$ as intramolecular and intermolecular proton transfer distortions and $A(8f)$ as out-of-plane molecular twisting (buckling) and π -bond switching of carboxylic groups. For each of them we have calculated the polarization by displacing *only* the atoms belonging to a given WP orbit and keeping the rest of them in their centrosymmetric positions, obtaining $\mathbf{P}_{4e} = (0.5, 0, -1.6)$, $\mathbf{P}_{4b} = (6.6, 0, -5.5)$ and $\mathbf{P}_{8f} = (5.5, 0, 0.4)$ $\mu\text{C}/\text{cm}^2$. Notably, their sum is $(12.6, 0, -6.7)$ $\mu\text{C}/\text{cm}^2$, which is almost equal to the total polarization $\mathbf{P}_{\text{tot}} = (12.7, 0, -6.6)$ $\mu\text{C}/\text{cm}^2$, calculated from the total polar distortion. The linearity of the partial polarizations is compatible with displacive-type ferroelectricity. Surprisingly, the mode decomposition shows that the $A(8f)$ mode makes almost as large a contribution as the intermolecular proton transfer in determining the total polarization. This effect can be related to a double(π)-bond switching of carboxylic $\text{C}=\text{O} \rightleftharpoons \text{C}-\text{O}$ bonds correlated with the intermolecular *and* intramolecular hydrogen distortion. This is shown in Fig. 4, where we present an enlarged view of the $A(8f)$ mode. In the upper part, we show the centric case, with hydrogens equidistant from nearest carbons or oxygens. In the lower part, we show the cooperative hydrogen distortions leading to the $+\mathbf{P}$ or $-\mathbf{P}$ state, which correlates, in turn, with the switching of double and single $\text{C}-\text{O}$ bonds and with the shortening and/or elongation of the corresponding $\text{C}-\text{O}$ bonds, in both $+\mathbf{P}$ and $-\mathbf{P}$. This picture is further confirmed by

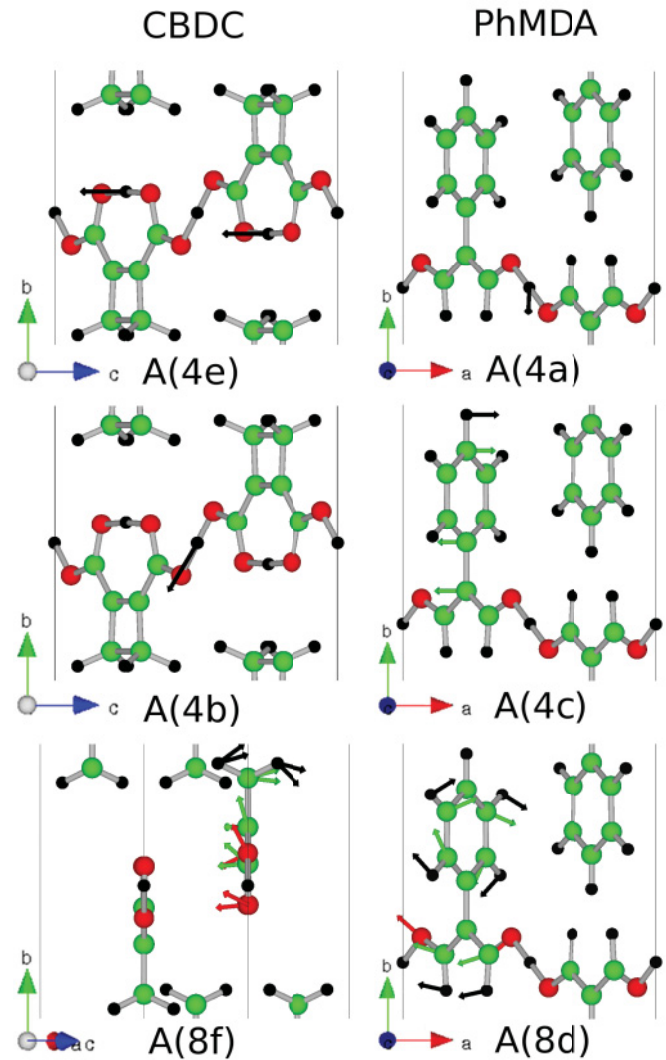


FIG. 3. (Color online) Displacements patterns (arrows) connecting centric to polar structures for atoms belonging to specified Wyckoff positions (top to bottom) for CBDC (left-hand side) and PhMDA (right-hand side).

the following computational experiment: (i) We first consider all the atoms at their centric positions (upper part in Fig. 4); (ii) we then move *only* the intramolecular *and* intermolecular hydrogen as, for instance, in the $+\mathbf{P}$ state, keeping all the other atoms fixed. The charge-density difference between (ii) and (i) shows a pileup of out-of-plane charge between $\text{C}_2=\text{O}_2$ and $\text{C}_1=\text{O}_3$, which corresponds to the incipient formation of the π (double) bonds. This can be easily seen in Fig. 5, where we highlight the charge-density difference isosurfaces between (ii) and (i) due to hydrogen displacements. In this case, these isosurfaces correspond to an increase of charge with respect to case (i): By moving *only* the intramolecular and intermolecular hydrogen atom, charge accumulates in regions of π -bond formation (see Fig. 4).

One could expect that the polar carboxylic groups, rather than the less polar $\text{C}-\text{C}$ bonds, might be responsible for the large polarization of the buckling mode. To confirm this, we have further extracted the contribution of the $\text{C}=\text{O}/\text{C}-\text{O}$ bonds to this polarization. The extracted polarization of

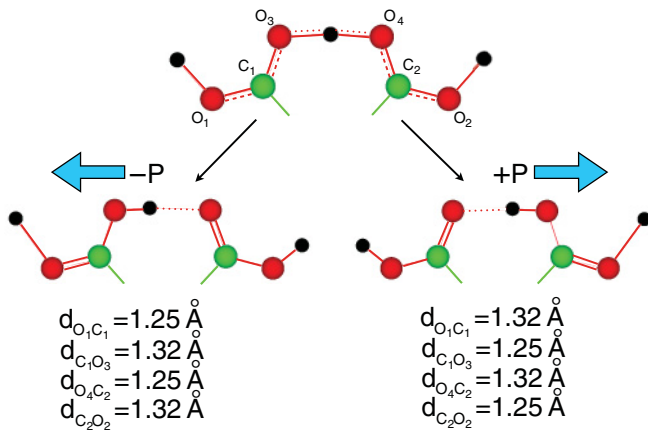


FIG. 4. (Color online) Switching between double and single bonds in the CBDC molecule. Top: centric case; bottom: switching between $+P$ and $-P$. The chemist convention for the orientation of the dipole moment is used here, i.e., the arrow starts at $\delta+$ and ends at $\delta-$.

(4.8, 0, -0.1) $\mu\text{C}/\text{cm}^2$ [versus the remaining contributions of (0.8, 0, 0.4) $\mu\text{C}/\text{cm}^2$] account for most of the large polarization of the **A(8f)** mode. Again linearity is well fulfilled. This clearly explains the origin of the surprisingly large polarization of the buckling mode. For PhMDA, we find partial modes **A(4a)**, **A(4c)**, and **A(8d)** whose contributions to the polarization are 5.8, 1.0, and 0.3 $\mu\text{C}/\text{cm}^2$ along the z polar axis, respectively. The linearity holds also in this case, but now the intermolecular proton transfer does give the dominant contribution.

Finally, for the centric structures, we have calculated the Born (or “dynamical” or “infrared”) charge tensors $Z_{k,\alpha\beta}^* = (\Omega/e)\partial P_\alpha/\partial u_{k,\beta}$, where P_α is the component of the polarization in direction α and $u_{k,\beta}$ is the displacement of atom k in direction β , Ω is the primitive cell volume, and e is the charge quantum. In perovskite ABO_3 oxides the ferroelectric tendency is well known to be connected with the presence of anomalously large Born charges.^{22,23} It should be noted that in low-symmetry cases, as in the present study, the Born tensor is not symmetric in its Cartesian indices. Therefore, we have split the tensor into symmetric Z_S^* and antisymmetric Z_{AS}^* parts. In the following, we will focus on the former, and in particular, on its three eigenvalues $\lambda_1 > \lambda_2 > \lambda_3$, whose physical interpretation is straightforward. Furthermore, only the hydrogen Born tensors will be considered. We have also calculated the phonon frequencies at the Γ point; the

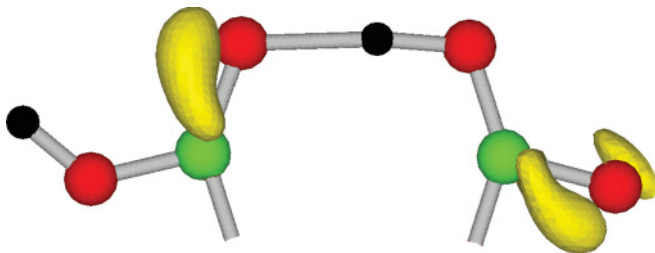


FIG. 5. (Color online) Difference between charge-density isosurfaces of structures shown in the upper and right-hand side bottom part of Fig. 4 (see text for details).

presence of an imaginary frequency usually implies a structural instability, in this case of the paraelectric structure.

Let us first consider CBDC. As expected, the significant deviations of the dynamical tensor with respect to the nominal charges involve the “active” H atoms. For the intermolecular hydrogen, $\lambda_{i,Z_S^*} = (3.4, 0.4, 0.1)$, and for the intramolecular hydrogen, $\lambda_{i,Z_S^*} = (2.2, 0.3, 0.3)$. The large values of the Born charges for hydrogens confirm their important contribution to the polarization, as found also in other hydrogen-bonded organic molecular crystals.^{43–45} The other hydrogens have only negligible absolute eigenvalues ~ 0.1 (some of them becoming negative). For the phonons, we found a large nondegenerate imaginary Γ phonon frequency of $\sim 106 \text{ cm}^{-1}$. According to a symmetry analysis,⁴⁶ infrared irreducible representations exist for *all* three WP positions with either A_u or B_u symmetry. This is not unexpected, as all WP positions carry a contribution to the polarization. In particular, the eigenvector of the imaginary frequency has symmetry B_u , which is *polar*. After normalization to 1 \AA , we use the AMPLIMODE software for studying the corresponding displacement pattern. The largest absolute $|u|$, where u is the displacement of the atom according to the phonon eigenvector, is 0.29 and 0.35 \AA for intramolecular and intermolecular hydrogens. Again, this confirms the dominant role of the two types of hydrogen in the ferroelectric properties. For the case of PhMDA, we found significant deviations of the dynamical charge tensor for intermolecular hydrogen, whose eigenvalues are $\lambda_{i,Z_S^*} = (4.1, 0.4, 0.2)$. The eigenvalues for other hydrogen atoms are smaller than 1. Finally, the imaginary phonon frequency is 112 cm^{-1} with *polar* symmetry B_u . Also in this case, the polarization vector of the eigenmode has a large displacement of $\sim 0.43 \text{ \AA}$ for the intermolecular hydrogen.

To summarize, we have studied the origin of ferroelectricity in CBDC and PhMDA using first-principles calculations and symmetry analysis methods. The estimated polarizations are as large as $\sim 14 \mu\text{C}/\text{cm}^2$ for CBDC and $\sim 7 \mu\text{C}/\text{cm}^2$ for PhMDA. We have shown that a partial mode analysis is a useful tool for exploring the polarization mechanisms. In both compounds, the proton transfer between (or within) molecular units appears to be the main contribution, as confirmed by the large dynamical charges and the analysis of the eigenmode displacement patterns. However, other contributions, especially the π -bond switching of carboxylic groups in CBDC, may also have a significant weight in the final polarization. Again, partial mode analysis has been used to elucidate the origin of the unexpectedly large contribution. We hope that our study will stimulate further attempts to search for new organic ferroelectrics with potentially large electric polarizations.

The work is supported by the European Research Council, 7th Framework Programme–FP7 (2007–2013)/ERC Grant Agreement No. 203523 and partly supported by the FIRST program from JSPS. Computational support by CASPUR Supercomputing Center in Rome is gratefully acknowledged. D.V. acknowledges support of ONR Grant No. N-00014-05-1-0054. S.H. acknowledges the support by KAKENHI (20110003) and the Sumitomo Foundation. A.S. thanks J. M. Perez-Mato, E. Tasci, D. Orobengoa, H. Stokes, and I. Baburin for useful discussions about symmetry aspects of the study.

*alessandro.stroppa@spin.cnr.it

- ¹P. Hlänggi, *Nat. Mater.* **10**, 6 (2011).
- ²J. Valasek, *Phys. Rev.* **15**, 537 (1920).
- ³G. Bush and P. Scherrer, *Naturwissenschaften* **23**, 737 (1935).
- ⁴G. Bush, *Helv. Phys. Acta* **11**, 269 (1938).
- ⁵S. Koval, J. Kohanoff, R. L. Migoni, and E. Tosatti, *Phys. Rev. Lett.* **89**, 187602 (2002).
- ⁶H. H. Wieder, *Phys. Rev.* **99**, 1161 (1955).
- ⁷Q. Ling, D. Liaw, C. Zhu, D. Chan, E. Kang, and K. Neoh, *Prog. Polym. Sci.* **33**, 917 (2008).
- ⁸R. C. G. Naber, K. Asadi, P. W. M. Blom, D. M. de Leeuw, and B. de Boer, *Adv. Mater.* **22**, 933 (2010).
- ⁹H. Ishizuka, Y. Motome, N. Furukawa, and S. Suzuki (2006) [<http://arXiv.org/pdf/1105.4247v1>].
- ¹⁰S. Horiuchi, Y. Tokunaga, G. Giovannetti, S. Picozzi, H. Itoh, R. Shimano, R. Kumai, and Y. Tokura, *Nature (London)* **463**, 789 (2010).
- ¹¹D. Braga, L. Maini, and F. Grepioni, *Cryst. Eng. Commun.* **3**, 27 (2001).
- ¹²S. Horiuchi and Y. Tokura, *Nat. Mater.* **7**, 357 (2008).
- ¹³A. Stroppa, P. Jain, P. Barone, M. Marsman, J. Perez-Mato, A. Cheetham, H. Kroto, and S. Picozzi, *Angew. Chem.* **50**, 5847 (2011).
- ¹⁴P. Jain, V. Ramachandran, R. J. Clark, H. D. Zhou, B. H. Toby, N. S. Dalal, H. W. Kroto, and A. K. Cheetham, *J. Am. Chem. Soc.* **131**, 13625 (2009).
- ¹⁵F. Kagawa, S. Horiuchi, M. Tokunaga, J. Fujioka, and Y. Tokura, *Nat. Phys.* **6**, 169 (2010).
- ¹⁶D. Belluš, H.-C. Mez, and G. Rihs, *J. Chem. Soc., Perkin Trans. II*, 884 (1974).
- ¹⁷D. Semmingsen, *Acta Chem. Scand. B* **31**, 114 (1977).
- ¹⁸S. Horiuchi, R. Kumai, and Y. Tokura, *Adv. Mater. (Weinheim, Ger.)* **23**, 2098 (2011).
- ¹⁹G. Kresse and J. Furthmüller, *Phys. Rev. B* **54**, 11169 (1996).
- ²⁰P. E. Blöchl, *Phys. Rev. B* **50**, 17953 (1994).
- ²¹J. P. Perdew, M. Ernzerhof, and K. Burke, *J. Chem. Phys.* **105**, 9982 (1996).
- ²²R. D. King-Smith and D. Vanderbilt, *Phys. Rev. B* **47**, 1651 (1993).
- ²³R. Resta, M. Posternak, and A. Baldereschi, *Phys. Rev. Lett.* **70**, 1010 (1993).
- ²⁴J. Paier, R. Hirschl, M. Marsman, and G. Kresse, *J. Chem. Phys.* **122**, 234102 (2005).
- ²⁵J. Paier, M. Marsman, K. Hummer, G. Kresse, I. C. Gerber, and J. G. Angyan, *J. Chem. Phys.* **124**, 154709 (2006).
- ²⁶J. Heyd, G. E. Scuseria, and M. Ernzerhof, *J. Chem. Phys.* **118**, 8207 (2003).
- ²⁷M. Marsman, J. Paier, A. Stroppa, and G. Kresse, *J. Phys. Condens. Matter* **20**, 064201 (2008).
- ²⁸A. Stroppa and S. Picozzi, *Phys. Chem. Chem. Phys.* **12**, 5405 (2010).
- ²⁹A. Stroppa and G. Kresse, *Phys. Rev. B* **79**, 201201 (2009).
- ³⁰C. Franchini, G. Kresse, and R. Podloucky, *Phys. Rev. Lett.* **102**, 256402 (2009).
- ³¹C. Franchini, T. Archer, J. He, X.-Q. Chen, A. Filippetti, and S. Sanvito, *Phys. Rev. B* **83**, 220402 (2011).
- ³²K. Hummer, J. Harl, and G. Kresse, *Phys. Rev. B* **80**, 115205 (2009).
- ³³D. Scanlon and G. Watson, *Chem. Mater.* **21**, 5435 (2009).
- ³⁴D. O. Scanlon, B. J. Morgan, G. Watson, and A. Walsh, *Phys. Rev. Lett.* **103**, 096405 (2009).
- ³⁵D. Scanlon, A. Walsh, and G. Watson, *Chem. Mater.* **21**, 4568 (2009).
- ³⁶S. Grimme, *J. Comput. Chem.* **27**, 1787 (2006).
- ³⁷T. Bucko, J. Hafner, S. Lebegue, and J. G. Angyan, *J. Phys. Chem. A* **114**, 11814 (2010).
- ³⁸D. Di Sante, A. Stroppa, and S. Picozzi (unpublished).
- ³⁹E. Kroumova, M. I. Aroyo, J. M. Perez-Mato, S. Ivantchev, J. M. Igartua, and H. Wondratschek, *J. Appl. Crystallogr.* **34**, 783 (2001).
- ⁴⁰Centric structures have been obtained by using the PSEUDOSYMMETRY software (Ref. 39), a computer program useful for predicting the high-symmetry structure based on the low-symmetry structure.
- ⁴¹J. M. Perez-Mato, D. Orobengoa, and M. I. Aroyo, *Acta Crystallogr. Sect. A* **66**, 558 (2010).
- ⁴²B. J. Campbell, H. T. Stokes, and D. E. Tanner, *J. Appl. Crystallogr.* **39**, 607 (2006).
- ⁴³G. Colizzi, J. Kohanoff, J. Lasave, and R. L. Migoni, *Ferroelectrics* **401**, 200 (2010).
- ⁴⁴S. Koval, J. Kohanoff, J. Lasave, G. Colizzi, and R. L. Migoni, *Phys. Rev. B* **71**, 184102 (2005).
- ⁴⁵F. Ishii, N. Nagaosa, Y. Tokura, and K. Terakura, *Phys. Rev. B* **73**, 212105 (2006).
- ⁴⁶E. Kroumova, M. I. Aroyo, J. M. Perez-Mato, A. Kirov, C. Capillas, S. Ivantchev, and H. Wondratschek, *Phase Transitions* **76**, 155 (2003).